International Journal of Biological Macromolecules 150 (2020) 595–604

Contents lists available at ScienceDirect

International Journal of Biological Macromolecules

journal homepage: http://www.elsevier.com/locate/ijbiomac

Chitosan-based biodegradable active food packaging film containing Chinese chive (*Allium tuberosum*) root extract for food application

Asad Riaz [a], Camel Lagnika [a], Hao Luo [a], Zhuqing Dai [a], Meimei Nie [a], Malik Muhammad Hashim [b], Chunquan Liu [a], Jiangfeng Song [a,*], Dajing Li [a,*]

[a] Institute of Agro-product Processing, Jiangsu Academy of Agricultural Sciences, Nanjing 210014, Jiangsu, China
[b] Department of Food Science and Technology, Gomal University, Dera Ismail Khan, Pakistan

ARTICLE INFO

Article history:
Received 27 December 2019
Received in revised form 3 February 2020
Accepted 9 February 2020
Available online 10 February 2020

Keywords:
Chinese chive root
Polyphenols
Antioxidant
Chitosan film
Active packaging

ABSTRACT

The objective of the present study was to develop chitosan (CS) based novel functional films containing Chinese chive root extract (CRE) using solution casting method. CRE at different concentrations (1, 3 and 5% in w/w) were incorporated into the film-forming solution. Scanning electron microscopy (SEM), Fourier transform-infrared spectroscopy (FT-IR), X-ray diffraction (XRD) and thermal behavior analysis (DSC & TGA) were performed to investigate the structure, potential interaction and thermal stability of prepared films. It was revealed by SEM that higher extract concentration triggered the formation of agglomerates within the films. Incorporation of CRE into CS resulted in decrease tensile properties of the films from 28.9 to 15.4 MPa, whereas thickness was increased from 0.076 to 0.113 mm. The water solubility, swelling degree and water vapor permeability were significantly decreased from 31.6 to 18.7%, 57.4 to 40.5% and 15.67 to 7.81 $\times 10^{-11}$ g·m^{-1}s^{-1}Pa^{-1}, respectively. DPPH and ABTS radical scavenging ability of CS-CRE films were increased from 6.95 to 47.05% and 11.98 to 57.38%, respectively. CS-CRE5 film showed the highest biodegradability of 47.36%. The films prepared by addition of CRE into CS exhibited good antioxidant and antimicrobial activity indicating that it could be developed as bio-composite food packaging material for food industry.

1. Introduction

Excessive use of petroleum-based plastic materials poses severe environmental problems due to their non-degradable nature [1]. These plastic materials generally pile up in landfills or in the oceans and increase eco-pollution [2]. Moreover, these plastic materials negatively affect consumer health. The most recent study stated the consumption of 39,000 to 52,000 particles of micro-plastics by humans annually [3]. Consequently, scientists have successfully developed food packaging films based on different biopolymers like protein, polysaccharides and lipids. These bio-based films have gained amicable attention not only as biodegradable material but also as a carrier of bioactive compounds [4,5].

Active packaging is a modern approach and has emerged as an attractive solution for food packaging film containing active compounds like antioxidants and antimicrobials [6]. Several natural ingredients such as red grape extract [7], grape seed extract, murta leaf extract, thyme extract, mango kernel extract [8], mango peel extract [6], tea polyphenols [9] and sweet potato extract [10] have been studied to improve the antioxidant properties of bio-based films. The fruit and vegetable processing industry produces a huge quantity of food waste which could be a promising source of polyphenols and other bioactive compounds [11].

Chitosan (CS) composed of D-glucosamine and *N*-acetyl-D-glucosamine monomers linked by β-(1 → 4), is a linear cationic polysaccharide [12]. Though CS has been attempted as food packaging material, yet its low antimicrobial and antioxidant potential make it unsuitable for active food packaging system [13]. To overcome these shortfalls, several natural plants extract having good bioactivities such as sweet potato extract [10] soybean seed coat extract [14] grape seed extract [15] olive pomace [16] and apple peel polyphenols [17] have been incorporated into CS film. Chinese chives (*Allium tuberosum*) belong to the *Liliaceae* family. It is widely grown as a commercial crop throughout Eastern and Southeast regions. The leaves and stem of the plant are not only used for culinary purposes but also for medical treatments of various ailments [18]. The biological functions and health benefits of Chinese chives are related to phytochemicals mainly polyphenols, sulfur-containing compounds and saponins [19].

The main phenolic compounds present in chives are gallic acid, catechin, p-coumaric acid, ferulic acid, isoquercetin and rutin [20,21]. The chives are used on a daily basis in almost every home in China, and thus produce a huge amount of waste in the form of roots. The chives roots are also a good source of antioxidants, like polyphenols, and

* Corresponding authors.
E-mail addresses: songjiangfeng102@163.com (J. Song), lidajing@163.com (D. Li).

https://doi.org/10.1016/j.ijbiomac.2020.02.078
0141-8130/

antimicrobial compounds [22]. Sulfur-containing compounds mainly allyl methyl sulfide and diallyl disulfide contribute to the antimicrobial activity of chives root extract [23]. Taking this into account, attention should be paid to Chinese chives root extract (CRE) as an active ingredient for the production of CS-based active packaging film. Chinese chives root is regarded as a waste and offers excellent antimicrobial and antioxidant properties. Therefore, the present study was planned to develop novel CS-based active food packaging film by the addition of Chinese chives root extract (CRE) and to evaluate the physical, mechanical, structural and biological activities of developed films. The prepared films were also evaluated as an oil storage packaging material for their potential application in the food industry.

2. Materials and methods

2.1. Materials and reagents

Chitosan having a degree of deacetylation of 80–95% and molecular weight 4×10^5 Da was supplied by Sinopharm Chemical Reagent Co. Ltd., China. Glycerol was procured from Solarbio Science & Technology Co., Ltd. (Beijing, China). 2,2-diphenyl-1-picrylhydrazyl (DPPH), Gallic acid (GA) and 2,2′-azino-bis-(3-ethylbenzothiazoline-6-sulphonic acid) (ABTS) were acquired from Sigma Chemical Co., Ltd. (St. Louis, MO, USA). Folin-Ciocalteau reagent was purchased from Kayon Biological Technology Co., Ltd. (Shanghai, China). All reagents used were of analytical grade.

2.2. Preparation of Chinese chive root extract

Fresh Chinese chives were obtained from a local vegetable market in Nanjing, China. Roots were carefully separated, thoroughly washed to remove soil particles and immediately placed in a conventional hot air oven for drying at 40 °C for 48 h. After that, a kitchen-type grinder (MJ-M176P, Panasonic, Japan) was used to crush the roots into powder. Extraction was then performed using the ultrasonic bath (KQ5200DE, Kunshan Co., Jiangsu, China). Briefly, 2 g sample of chive root powder was extracted with 50 mL of 80% ethanol solution for 30 min at 25 °C. The chive root extract was obtained after filtration under vacuum and concentrated using a rotary evaporator.

2.3. Chemical composition of CRE

2.3.1. Determination of total polyphenols content

Folin-Ciocalteu method reported by Saeeduddin et al. [24] using GA as a standard, was used to determine the total polyphenols contents in CRE. Briefly, the sample (0.5 mL) was mixed with Folin-Ciocalteu reagent (1.0 mL, 10 times diluted) and kept for 6 min in the dark. After adding 2 mL sodium carbonate solution (20 g/100 mL), the mixture was incubated for 60 min at 30 °C. The absorbance was measured at 750 nm and the results were expressed as mg of GA equivalent (GAE/mg DW). All experiments were replicated thrice.

2.3.2. HPLC analysis of the phenolic composition, ascorbic acid, and alliin

The phenolic composition of CRE was determined by the Agilent 1200 series HPLC system (Agilent Technologies, Santa Clara, CA, USA) equipped with autosampler and diode array detector set at a wavelength of 280 and 320 nm. The separation was achieved by Eclipse XDB C18 (4.6 × 250 mm, 5 μm) column set at 35 °C and sample injection volume was 20 μL filtered with 0.45 μm membrane filter (Millipore, USA). A binary mobile phase consisted of (A) aqueous formic acid (0.1% v/v) and methanol (B) pumped at flow rate of 0.6 mL/min for 55 min with following gradient conditions: 0 min, 5% B; 40 min, 45% B; 45 min, 45% B, 55 min, 5% B. The eluted peaks were identified with commercially available standards of phenolic compounds. For ascorbic acid determination, an isocratic mobile phase consisting of aqueous 0.2% (v/v) metaphosphoric acid with a flow rate of 0.8 mL/min, injection volume 20 μL and detection wavelength 240 nm was used. The L-ascorbic acid was determined by a comparison with the standardized retention time matching with the UV absorption spectrum. For alliin determination, the mobile phase used was methanol: water (95:5) with 0.8 mL/min flow rate and detection wavelength was set at 214 nm. The alliin content was determined by the standard solution of alliin. All experiments were performed in triplicate.

2.4. Film production

CS film-forming solution was prepared by mixing CS (2%, w/v) in acetic acid aqueous solution (1.0%, v/v) with stirring (800 rpm) for 4 h. Glycerol (30%, w/w) was added as a plasticizer into CS film-forming solution with further stirring for 0.5 h. After that different concentrations of CRE (1, 3 and 5% hereafter referred to as CRE1, CRE3, and CRE5, respectively) based on the weight of CS were added into the CS film-forming solutions with continuous stirring for 0.5 h. The control CS film was prepared in the absence of CRE. Air bubbles from film-forming solutions were removed through vacuum degasification for 1 h. Lastly, the CS-CRE solutions with the same quantity (70 mL) were poured into Petri dishes of 15 cm diameter for 48 h at 25 °C. The CS-CRE films were carefully removed and conditioned in a humidity chamber at 25 °C and 52% RH for 48 h for further experiments.

2.5. Characterization of CS-CRE films

2.5.1. Scanning electron microscopy

The film surface and cross-section morphological structure were observed with a scanning electron microscopy (SEM, Carl Zeiss EVO-LS-10, Germany) at 10 kV. Pieces of the films (5 × 5 mm) were cut, dried and mounted on aluminum stubs using double-sided carbon tape and sputter-coated with gold.

2.5.2. Fourier transform-infrared spectrometry

Fourier Transform-Infrared (FT-IR) spectrometry was applied to study the preliminary structures of the prepared films by FT-IR spectrometer (Nicolet iS-50, Thermo, USA). The FT-IR spectra were recorded in the frequency range of 4000 to 400 cm^{-1}.

2.5.3. X-ray diffraction

X-ray diffractometer (D8 Advance, Bruker, USA) was used to explore the crystal structures of films at a voltage of 40 kV and 100 mA. The scattered radiation was detected in the angular range $2\theta = 10–40°$ with a scanning speed of 5°/min.

2.5.4. Thermogravimetric analysis

Thermogravimetric analysis (TGA) was conducted using Pyris 1 TGA (Perkin Elmer, USA) over a temperature range of 25–600 °C at the rate of 10 °C/min under a dynamic nitrogen atmosphere. The film samples about 5 mg were put in sealed aluminum pans, and an empty pan was used as a reference.

Table 1
Chemical composition of chive root extract.

Compound	Retention time (min)	Content (μg/g dw)
Gallic acid	12.11	129 ± 2.58
Catechin	15.63	237 ± 4.74
Caffeic acid	20.04	392 ± 7.84
Epicatechin	21.75	128 ± 2.56
Chlorogenic acid	23.59	341 ± 6.82
Ferulic acid	36.10	249 ± 4.98
Kaemferol	37.21	187 ± 3.74
Rutin	40.36	172 ± 3.44
Ascorbic acid	3.86	213 ± 4.26
Alliin	3.01	419 ± 6.48

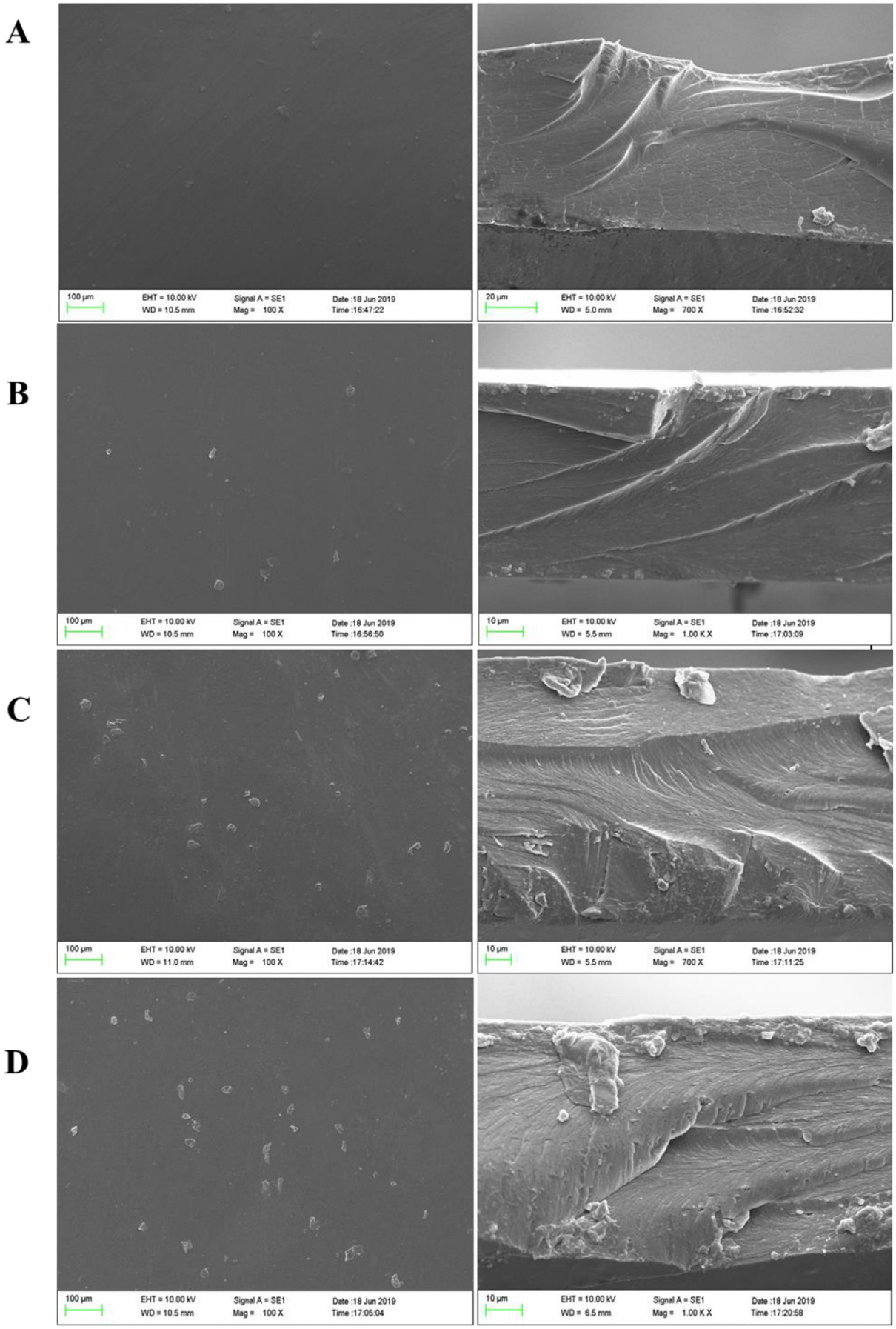

Fig. 1. SEM surface and cross section micrographs of CS-CRE films. (A), Control film with 0% CRE; (B), film with 1% CRE; (C), film with 3% CRE; (D), film with 5% CRE.

2.5.5. Differential scanning calorimetry (DSC)

DSC analysis was performed using a Q1000 DSC system (TA instruments, USA). Film pieces (10 mg) were sealed in a standard aluminum pan heated at a constant rate of 10 °C/min from 0 to 450 °C at nitrogen atmosphere.

2.5.6. Film thickness measurement

A digital micrometer was used to measure the thickness of the prepared films at ten different positions and the average value was reported.

2.5.7. Determination of films solubility and swelling degree

Solubility and swelling degree of prepared films were determined by the method of Riaz et al. [17] with slight modification. The films pieces were cut into 2 × 2 cm dimensions and solubility was calculated using the following equation:

$$\text{Film solubility}\ (\%) = \frac{M1-M2}{M1} \times 100 \quad (1)$$

where ($M1$) is initial dry mass and ($M2$) is final dry mass after placing the films in 50 mL distilled water for 24 and dried at 105 °C. Following equation was used to calculate the swelling degree of films:

$$\text{Film swelling degree}\ (\%) = \frac{M2-M1}{M1} \times 100 \quad (2)$$

where ($M1$) is the initial weight of films and ($M2$) is the final weight of films after placing in 30 mL distilled water for 24 h.

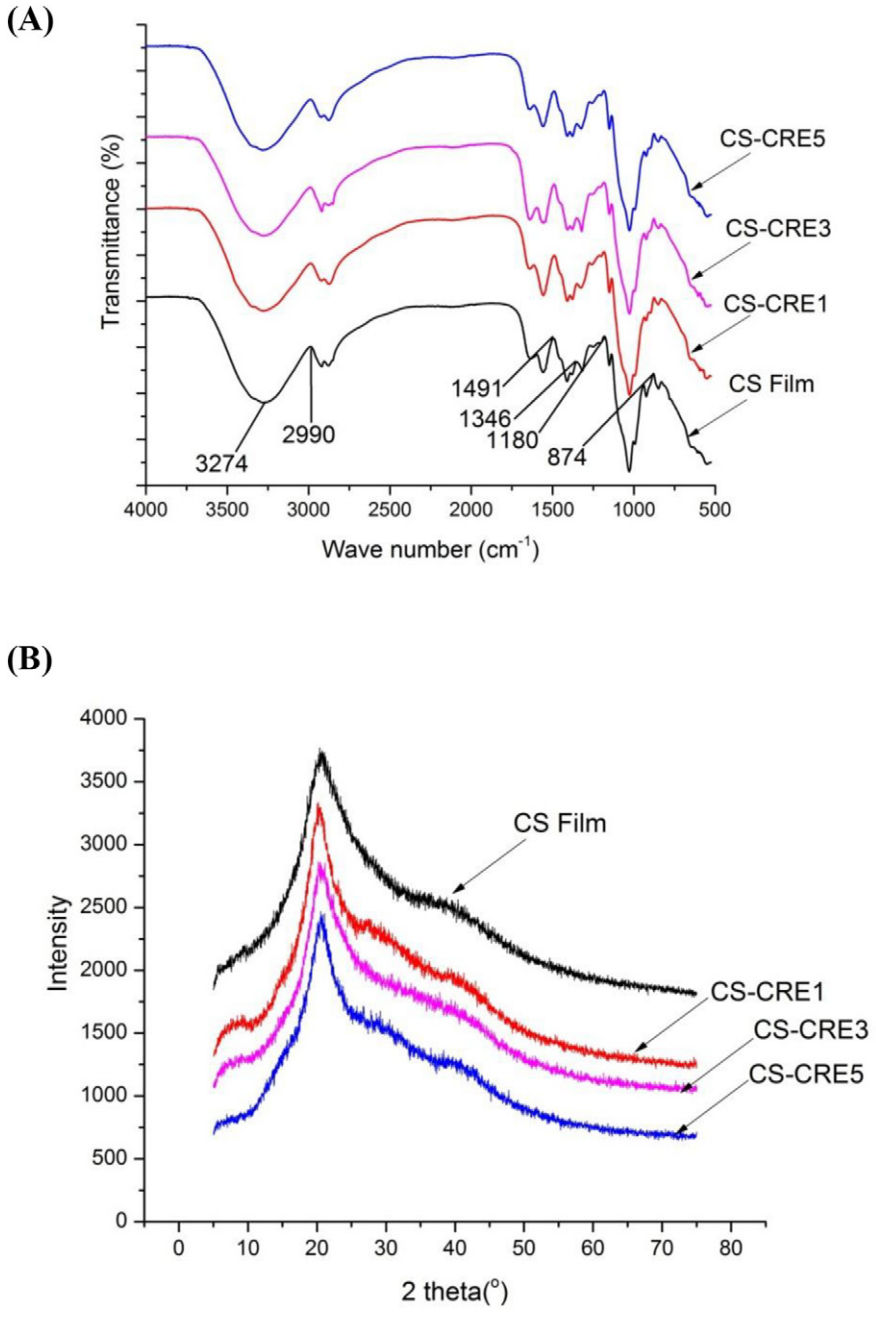

Fig. 2. FT-IR spectra of CS-CRE films (A) X-RD pattern of CS-CRE films (B).

2.5.8. Determinations of water vapor permeability and water content

To measure the water vapor permeability (WVP) of prepared films, the method described by Hassannia-Kolaee, Khodaiyan & Shahabi-Ghahfarrokhi [25] was used with a slight amendment. Special glass cups were taken with a diameter of 4 cm and filled with anhydrous calcium chloride and film samples (5 × 5 cm) were sealed on top of each glass cup. The cups were placed in a desiccator at 75% RH which was maintained by a saturated solution of sodium chloride. The glass cups were then weighed after every hour till the first 10 h and then after 24 h and slope of weight change against time was calculated using linear regression. The WVP was calculated by the following equation (g m^{-1} s^{-1} Pa^{-1}):

$$\mathrm{WVP} = \frac{\mathrm{Slope} \times \mathrm{L}}{\mathrm{A} \times \Delta \mathrm{P}} \tag{3}$$

where L is the average film thickness (m), A is the transfer area (m^2) and ΔP the partial water vapor pressure difference.

The moisture content of the films was determined by measuring the weight loss of the films upon drying in an oven at 105 ± 1 °C for 24 h. The moisture content was calculated according to following equation:

$$\text{Water content } (\%) = \frac{M1 - M2}{M1} \times 100 \tag{4}$$

where (*M1*) is the initial weight of films and (*M2*) is the dry weight of the films.

2.5.9. Film color, transmittance and opacity

The color of prepared films was determined by the CR-400 colorimeter (Konica Minolta, Japan). The white plate was used as a standard. (L^*), (a^*) and (b^*) values were noted to characterize the film color for lightness, red-green and yellow-blue in the Hunter Lab scale. Total color difference (ΔE), yellow index (YI) and white index (WI) was calculated using the following equations:

$$\Delta E = \sqrt{\left(L_i^* - L^*\right)^2 + \left(a_i^* - a^*\right)^2 + \left(b_i^* - b^*\right)^2} \tag{5}$$

$$\mathrm{YI} = \frac{142.86 \times b^*}{L^*} \tag{6}$$

$$\mathrm{WI} = 100 - \sqrt{(100 - L^*)^2 + a^{*2}} + b^{*2} \tag{7}$$

The transmittance and opacity of the prepared films were determined by the method of Riaz et al. [26] using a UV-6300 spectrophotometer (Mapada, China) at 600 nm. The film strips were cut into 1 × 4 cm length and transmittance was measured. The absorbance values were noted and the opacity was calculated using the following equation:

$$O = Abs_{600}/L \tag{8}$$

where, *O* is the opacity, Abs_{600} is the absorbance value at 600 nm and *L* is the film thickness (mm).

2.5.10. Mechanical properties of films

The mechanical properties of prepared films including tensile strength (TS) and elongation at break (EB) were determined by the method of Ferreira, Nunes, Castro, Ferreira & Coimbra [27] using a texture analyzer (TA. XT Plus, Stable Micro Systems, British). The films were cut into strips of 150 × 20 mm and positioned between the grips with 100 mm initial separation, 50 mm/min detector speed and load force Newton (N) was used. TS and EB were calculated based on the ASTM D 882–10 standard method.

2.5.11. Antioxidant activity of films

Antioxidant activity of the films was evaluated following the method described by Liu, Meng, Liu, Kan & Jin [28]. Film samples (5 mg) and 1.5 mL of ABTS working solution was mixed and absorbance was measured at 734 nm and scavenging activity was calculated using the following equation:

$$\text{Scavenging activity on ABTS free radicals } (\%) = \left(1 - \frac{A1 - A2}{Ao} \times 100\right) \tag{9}$$

where A_o is the absorbance of the initial $ABTS^+$, A_1 is the absorbance of the sample, and A_2 is the absorbance of the sample with PBS.

For DPPH radical scavenging activity determination film sample (5 mg) were mixed with methanolic DPPH solution (0.2 mM, 1.5 mL) and placed in the dark at 30 °C for 0.5 h and absorbance was measured at 517 nm. Following equation was used to calculate the scavenging activity:

$$\text{Scavening activity on DPPH free radicals } (\%) = \left(1 - \frac{A1 - A2}{Ao} \times 100\right) \tag{10}$$

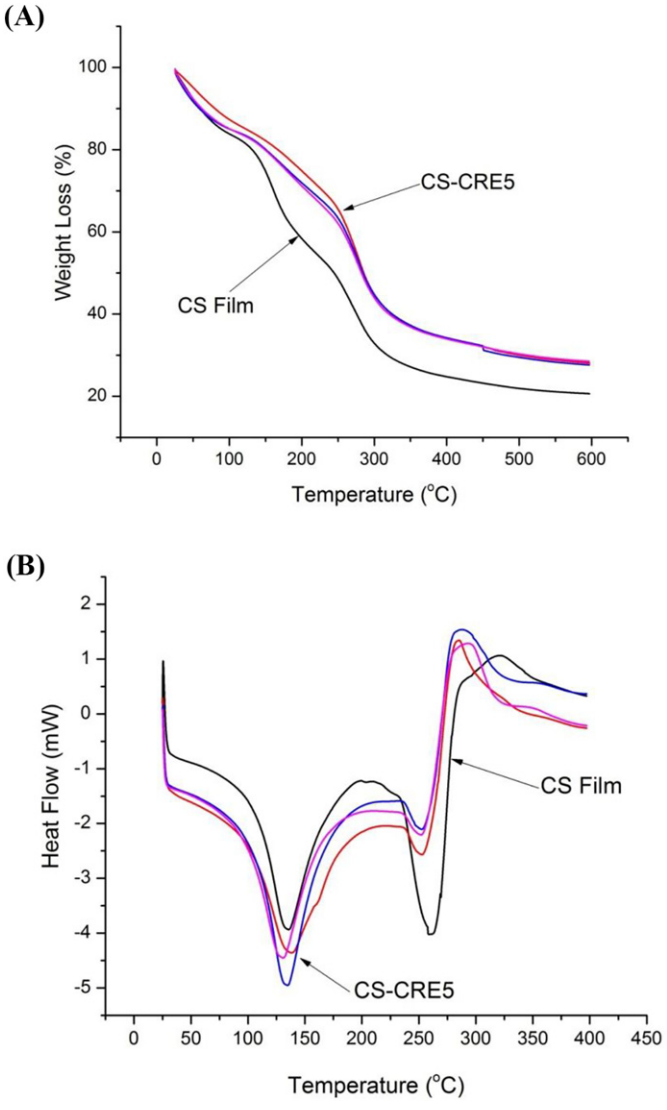

Fig. 3. TGA curves of CS-CRE films (A) DSC thermo-grams of CS-CRE films (B).

Table 2
Physical properties of CS-based CRE films.

Film sample	Thickness (mm)	Swelling degree (%)	Solubility (%)	Moisture content (%)	WVP ($\times 10^{-11}$ g^{-1} s^{-1} Pa^{-1})
CS	0.076 ± 0.0017^{a}	57.38 ± 1.14^{d}	31.60 ± 0.63^{d}	27.16 ± 0.54^{d}	15.67 ± 0.31^{d}
CS-CRE1	0.085 ± 0.0023^{b}	52.03 ± 1.04^{c}	28.14 ± 0.57^{c}	24.41 ± 0.48^{c}	13.27 ± 0.26^{c}
CS-CRE3	0.098 ± 0.005^{c}	46.42 ± 0.92^{b}	24.47 ± 0.49^{b}	20.66 ± 0.41^{b}	11.19 ± 0.22^{b}
CS-CRE5	0.113 ± 0.0020^{d}	40.49 ± 0.80^{a}	18.67 ± 0.37^{a}	17.72 ± 0.35^{a}	7.81 ± 0.15^{a}

Values are expressed as mean ± standard deviation. Different letters in the same column indicate significant differences ($p < 0.05$).

where A_o is the absorbance of the initial DPPH, A_1 is the absorbance of sample and A_2 is the absorbance of the sample with methanol.

2.5.12. Antimicrobial activity of films

The antimicrobial activity of the prepared films was determined according to the method described by Khalid et al. [29] against two Gram-positive *Bacillus cereus* (CGMCC 1.895), *Staphylococcus aureus* (CGMCC 1.8721) and two Gram-negative *Escherichia coli* (CGMCC 7.59), *Salmonella typhimurium* (CGMCC 1.10754) bacteria. Briefly, the bacterium suspension of 0.1 mL was prepared and the final concentration of 1.5–3.0 × 10^5 CFU/mL was obtained by diluting with 0.3 mM PBS (pH 6.8). The discs of films (diameter 1/4 10 mm) were prepared, sterilized under UV light and carefully placed into Petri dishes containing solid medium. After that, the prepared bacterium suspension of 0.1 mL was spread into each Petri plate followed by incubation at 37 °C for 24 h. The inhibition zone was calculated using a sliding caliper.

2.5.13. Biodegradation test

The biodegradation capacity of the prepared films was determined by the composting test as described in the literature [9]. The soil was procured from the experimental field of Jiangsu Academy of Agricultural Sciences (Nanjing, China). The soil was placed in a plastic tray in which samples of each film (2 × 2 cm) were buried at 2 cm depth for three weeks. The soil was sprayed by water two times a day. At the end of every week, the film samples were taken out and weight loss of each film was calculated.

2.6. Potential application on soybean oil packaging

2.6.1. Oil resistance ability of films

The oil resistance performance of the films was determined by the method of Wang et al. [14] with slight modifications. The filter paper (6 cm diameter) was dried to a constant weight in a hot air oven at 50 °C. Film samples (4 cm × cm) were fixed with ropes on the top of glass test tubes containing 5 mL of oil and were placed on the filter paper upside down for 48 h. The filter paper was weighed after 48 h and oil absorption rate (OAR) was calculated by the following equation:

$$OAR\ (\%) = (m - m_o)/m_o \times 100 \quad (11)$$

where m is the weight of filter paper after 48 h and m_o is the weight of dried filter paper.

2.6.2. Determination of peroxide value (POV)

Film samples were sealed with line rope on the top of glass bottles containing soybean oil and stored at 50 °C for 28 days. Sample of 5 mL was taken out from each glass tube on Day 1, 7, 14, 21, 28 to determine the POV according to the method of Firestone [30]. The analysis was performed in triplicate and average values were reported. A glass bottle without any film was used as a control.

2.7. Statistical analysis

Statistical analysis of all data was performed using statistical software SPSS 20.0. To assess the difference between factors and levels one-way Analysis of variance (ANOVA) was applied. Tukey's multiple range tests were used to know the significant differences between means and if $p < 0.05$, differences were considered to be significant.

3. Results and discussion

3.1. Total phenolic content and chemical composition of CRE

The total phenolic contents of chive roots extract were 321 ± 2.88 mg GAE/100 g dry weight. The chive root extract exhibited a good quantity of phenolic contents, which are in line with results reported earlier [31]. The phenolic composition of CRE was determined by HPLC using 12 commercially available standards and 8 compounds were identified according to retention time and are presented in Table 1. Moreover, ascorbic acid and alliin (sulfur-containing compound) were also present in CRE. These findings clearly show that the chives roots waste is a good source of polyphenols, ascorbic acid and alliin, which can be utilized to increase the bioactivities as well as for the production of CS-based biodegradable food packaging film.

3.2. Characterization of CS-CRE film

3.2.1. SEM

Structure, morphology, and homogeneity of the matrix play a vital role in the permeability of the films [32]. SEM images of surface and cross-section of CS and CS-based CRE films are shown in Fig. 1. SEM images indicate that the surface of the control film was quite smooth, uniform, ordered and in homogeneous structure without bubbles or porous. Similar findings have been reported by Sun et al. [33]. The presence of CRE in the composite films affected the structure of the films and caused discontinuities in the matrix polymer. At a low concentration of extract (CRE1%), most of the compounds were dispersed in matrix uniformly without any obvious aggregation. With the increase of CRE concentration from 1% to 5%, more and more white spots appeared and created the disturbance in the structure resulting in a more heterogeneous surface. This might be due to the hydrophilicity of polyphenolic

Table 3
Color, transmittance and opacity of CS-based films with different concentration of CRE.

Film sample	L*	a*	b*	ΔE	YI	WI	Transmittance (%)	Opacity (A. mm^{-1})
CS	88.27 ± 1.76^{d}	−1.17 ± 0.0^{a}	7.66 ± 0.15^{a}	9.30 ± 0.20^{a}	12.39 ± 0.24^{a}	85.94 ± 1.71^{a}	81.23 ± 1.62^{a}	0.64 ± 0.0^{a}
CS-CRE1	76.23 ± 1.52^{c}	4.38 ± 0.08^{b}	17.89 ± 0.35^{b}	25.13 ± 0.58^{b}	33.52 ± 0.67^{b}	69.92 ± 1.39^{b}	73.41 ± 1.46^{b}	1.16 ± 0.02^{b}
CS-CRE3	64.59 ± 1.29^{b}	14.63 ± 0.29^{c}	32.71 ± 0.65^{c}	45.89 ± 1.40^{c}	72.34 ± 1.44^{c}	49.62 ± 0.99^{c}	60.17 ± 1.20^{c}	2.03 ± 0.04^{c}
CS-CRE5	49.17 ± 1.03^{a}	20.98 ± 0.41^{d}	44.10 ± 0.88^{d}	65.80 ± 2.32^{d}	128.12 ± 2.56^{d}	29.51 ± 0.59^{d}	49.66 ± 0.99^{d}	3.21 ± 0.06^{d}

Values are expressed as mean ± standard deviation. Different letters in the same column indicate significant differences ($p < 0.05$).

compounds present in the extract. Similar findings were reported by Akhter et al. [34].

3.2.2. FT-IR

To explore the intermolecular changes between CS control film and CRE added CS films, FT-IR spectroscopy was performed and Fig. 2A shows the relevant spectra of each film. The spectral bands of all the tested films were appeared around 3274 cm^{-1} for O—H stretching, 2990 cm^{-1} for C—H stretching from alkyl groups and peaks at 1491, 1346,1180 and 874 cm^{-1} corresponded to C═O, N—H bending vibration, C—N stretching and C—O—C band stretching, respectively [35]. It is evident from the spectral peaks that there is no covalent bond between CS and CRE proving only physical interaction between filler and matrix [36]. Similarly, shifting to lower wavenumbers of some of the peaks has occurred with the increase of CRE concentration. This could be related to the existence of CRE, which changed the availability of OH group inside the polymer network due to intermingling with the glycerol-polymer matrix. These findings are in line with the results of Wang et al. [37].

3.2.3. XRD

To study the crystalline structure of the control CS film and to reveal the effect of incorporated CRE on control CS film XRD analysis was performed. The XRD spectrum of all the prepared films is shown in Fig. 2B. It is evident from the spectrum that CS has an almost amorphous structure with a broader and single peak appearance at the 2θ about 21°. Similar results have been reported by Wang et al. [37]. After the addition of CRE into CS control film, no change in the crystalline structure of CS control film was observed. This shows that the addition of CRE didn't change the internal structure of the CS control film at all. The X-ray spectrum of the films prepared by the addition of CRE only showed a decrease in the intensity of spectrum peaks and became sharper as the concentration of CRE increased to 5%. This process could be better described by the fact that interaction between CS and CRE decreased the formation of hydrogen bonds in CS itself, and thus resulted in decrease crystallinity. These findings are in compliance with previous reports [36,38].

3.2.4. TGA and DSC

TGA curves of CS-based CRE composite films incorporated with CRE at different concentrations are shown in Fig. 3A. The control CS film showed similar thermal behavior as reported earlier [10]. All the films exhibited mainly three weight loss stages. The first stage (40 to 120 °C) was associated with the loss of water due to breakdown of hydrogen bonding, the second stage (130 to 250 °C) was related to the decomposition of glycerol and third stage (260 to 400 °C) was ascribed to polymer decomposition and depolymerization. It is obvious from the findings that CS-CRE films exhibited strong thermal stability than that of CS control film. The weight loss of CS-CRE films was significantly lower than that of CS control film which proved that the incorporation of CRE into CS film increased the thermal stability of the native film. These findings are supported by the earlier reports [36,39]. A similar trend can be observed in Fig. 3B, which shows DSC curves with two main stages of mass loss for all samples. It is obvious from the results that the CS-CRE films exhibited a declining trend of peak temperature and increasing peak area, resulting in higher thermal stability. The finding of both DSC and TGA implies that as the concentration of extract was increased in the CS matrix, it increased the thermal stability of the films.

3.3. Physical properties of CS-CRE film

3.3.1. Thickness

The thickness of the prepared films is presented in Table 2 and it increased ($p < 0.05$) as the concentration of CRE was increased in CS film. This might be due to the interactions between polyphenols and CS, which resulted in tighter binding of polyphenols and CS [40]. The presence of polyhydroxyl in CS structure resulted in the narrow distance between CS molecules, and made the structure of film more compact and increased thickness. Similar findings have been reported previously [37,41].

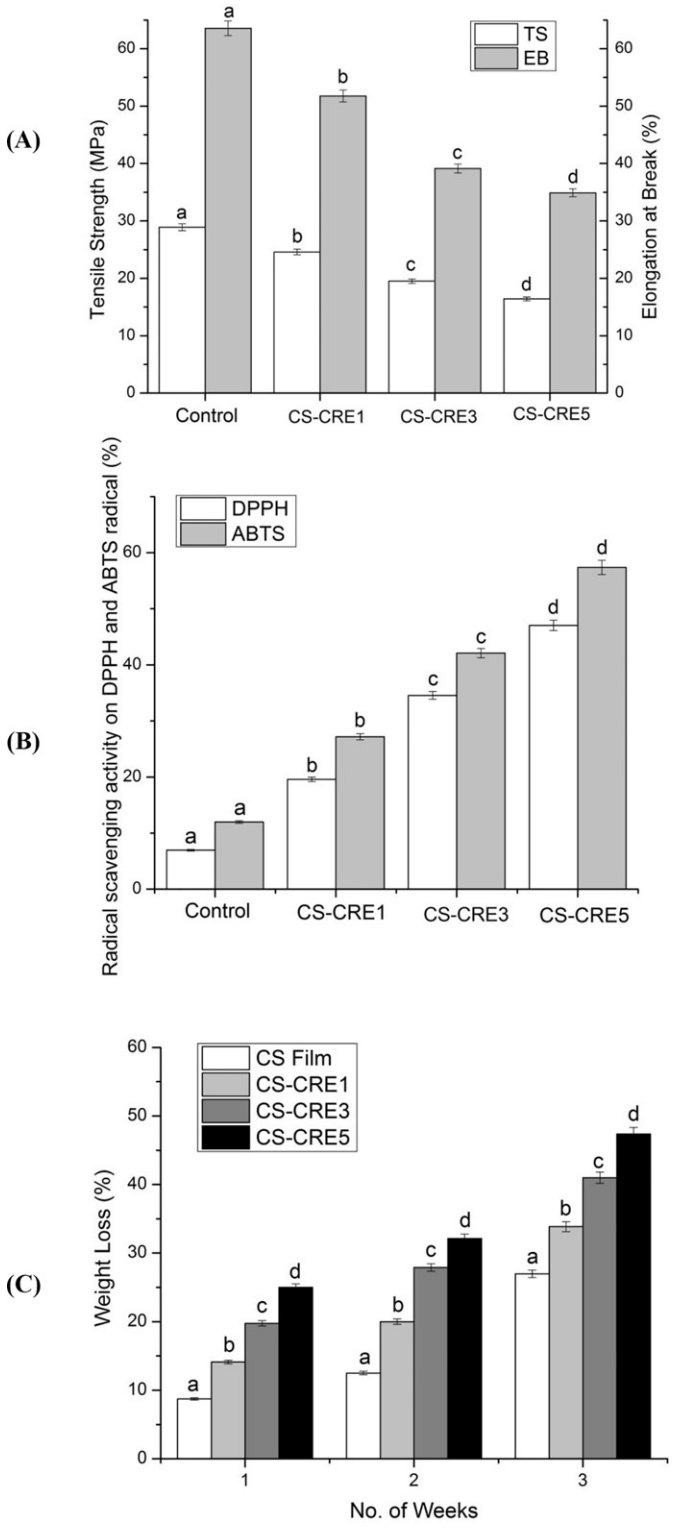

Fig. 4. Mechanical properties of CS-based films with different concentrations of CRE (A). Values are mean ($n = 3$) ± SD, and a–d represent significant differences ($p < 0.05$) in the same band. Scavenging activities of the CS-CRE films on DPPH and ABTS radicals (B). Biodegradability evaluation of CS-CRE films (C). Different letters indicate significant differences ($p < 0.05$).

Table 4
Inhibitory effects of CS-based film with different concentrations CRE on four kinds of bacteria.

Film samples	Inhibition zone diameter (mm)			
	E. coli	*B. cereus*	*S. aureus*	*S. typhimurium*
CS	4.43 ± 0.08[a]	6.21 ± 0.12[a]	7.13 ± 0.14[a]	4.11 ± 0.08[a]
CS-CRE1	7.18 ± 0.14[b]	11.83 ± 0.23[b]	10.64 ± 0.21[b]	6.87 ± 0.13[b]
CS-CRE3	12.87 ± 0.25[c]	15.39 ± 0.30[c]	14.73 ± 0.29[c]	11.54 ± 0.23[c]
CS-CRE5	16.21 ± 0.32[d]	18.79 ± 0.37[d]	18.12 ± 0.36[d]	14.91 ± 0.29[d]

Values are expressed as mean ± standard deviation. Different letters in the same column indicate significant differences ($p < 0.05$).

3.3.2. Swelling degree, water solubility and moisture content

The water resistance behavior of a film is greatly influenced by the higher or lower values of swelling degree and water solubility, respectively [32]. The results of moisture-related properties are presented in Table 2 and a decrease ($p < 0.05$) can be seen in swelling degree and water solubility for the CS-CRE films. The existence of hydrophilic groups like hydroxyl groups in the CS molecule is mainly responsible for its intrinsic swelling behavior [42]. It is evident from the results that a higher concentration of CRE decreased the water solubility of CS-CRE films. This could be better explained by the formation of strong hydrogen bonds between the CS matrix and the polyphenolic compounds present in the extract. Similar behavior for moisture content of the CS-CRE films also observed after increasing the concentration of CRE into CS film. Similar results have been reported by Uranga et al. [43] and Rui et al. [44].

3.3.3. WVP

The WVP experiment was performed to observe the moisture permeability behavior of the prepared films and results are presented in Table 2. The control CS film showed the highest value of WVP, which is 15.67×10^{-11} g·m^{-1}s^{-1}Pa^{-1}. The addition of 1 to 5% CRE into CS films decreased ($p < 0.05$) the WVP to 7.81×10^{-11} g·m^{-1}s^{-1}Pa^{-1}. The possible reason behind this reduced WVP is limited interaction between water molecules present in the film due to the cross-linking effect between CS, glycerol and CRE resulting in less availability of free water [45]. The low value of WVP for food packaging films is highly desirable to prevent the moisture transfer between food and the surrounding environment. The thickness of the films also plays a vital role in determining the water barrier properties. Films with higher thickness have low WVP value because it would take a longer time for water molecules to pass through the film. Kurek et al. [46] also reported similar behavior after the incorporation of blue and blackberry extract into CS-based films.

3.3.4. Color, opacity and transmittance

The consumer preference is greatly influenced by the color and opacity of the food packaging materials. The color values of all the tested films YI, ΔE and WI, as well as opacity and transmittance, are presented in Table 3. The control films were highly transparent and with slightly yellow color; however, changes in color were observed with the addition of CRE into CS. A marked difference ($p < 0.05$) was observed among all the a^*, b^* and L^* values. The color of the film became darker and more yellowish when the concentration of CRE was increased to 5%. Film transmittance was also decreased ($p < 0.05$) with the increase of CRE concentration. The improvements in color attributes and decreasing tendency towards transmittance in CS-CRE films would be useful to protect food against discoloration, off-flavor and nutrient loss [47]. Similar findings have been reported earlier by Wang et al. [48].

3.4. Mechanical property of CS-CRE film

The results of mechanical properties for all the prepared films are depicted in Fig. 4A. A decrease ($p < 0.05$) in TS and EB can be seen in all the tested films. It is obvious from the figure that CS control film showed the highest strength of mechanical properties, whereas the presence of CRE in the CS matrix decreased the mechanical properties of CS control film. TS and EB values of CS control films were 28.89 MPa and 63.56%, respectively, whereas for CS-CRE5, these values were reported to be 16.41 MPa and 34.91%, respectively. The results showed a gradual decrease in the film strength of CS-CRE films. Similar results have been reported previously [17,49]. The mechanical strength of a film strongly depends upon polymer composition, intra-molecular forces, and the presence of crystallites as well as microstructure of the film network [50]. It is evident from the structural analysis like SEM and XRD of all the films that as the concentration of CRE was increased in CS matrix, it created more aggregation and decreased the crystalline structure of CS control films. Therefore, it can be concluded that the addition of CRE into CS control film disturbs the crystalline order and prevents the inter-chain interaction of polymer, resulting in decreased mechanical properties of the CS-CRE films [33].

3.5. Bioactivities of CS-CRE film

3.5.1. Antioxidant activity

The main attribute of an active food packaging film is its antioxidant potential [51]. DPPH and ABTS radical scavenging ability of all the prepared films is depicted in Fig. 4B. Antioxidant activity of CS-CRE films was enhanced ($p < 0.05$) by the addition of CRE. A similar increase in antioxidant activity was seen when honeysuckle flower extract and mango leaf extract were added into CS films, respectively [52,53]. The possible explanation of increased antioxidant activity is the presence of phenolic groups in CRE [54]. The total phenolic contents were increased with increasing concentration of CRE in CS-CRE films. A similar trend of improved antioxidant activity was reported with CS film β-Carotene loaded starch nanocrystals [55].

3.5.2. Antimicrobial activity

The active food packaging film should possess good antimicrobial activity to protect the food from microbial growth and preserve it for an extended period of time [56]. Two Gram-positive (*B. cereus* and *S. aureus*) and two Gram-negative (*E. coli* and *S. typhimurium*) bacteria were used to assess the antimicrobial activity of all the prepared films. As presented in Table 4, the CS-CRE films exhibited inhibitory effects ($p < 0.05$) on both Gram-positive and Gram-negative bacteria and inhibitory zones were increased with increasing concentration of CRE into CS control film. The antimicrobial ability of CS films was due to increased cellular permeability caused by the interactions between CS and

Table 5
Oil absorption ratio (OAR %) of CS- CRE films and POV (mEq/kg) of soybean oil stored in CS-CRE films.

Film samples	OAR	POV				
		DAY 1	DAY 7	DAY 14	DAY 21	DAY 28
Open control	–	2.19 ± 0.02 [a]	8.61 ± 0.29[a]	17.89 ± 0.55[a]	41.12 ± 1.08[a]	63.21 ± 1.38[a]
CS film	0.32 ± 0.006[a]	2.31 ± 0.05 [a]	6.43 ± 0.23[b]	15.59 ± 0.42 [b]	31.89 ± 0.79[b]	46.31 ± 1.03[b]
CS-CRE1	0.28 ± 0.005[b]	2.65 ± 0.03 [a]	4.81 ± 0.11[c]	13.19 ± 0.21[c]	26.31 ± 0.36[c]	37.49 ± 0.46[c]
CS.CRE3	0.17 ± 0.002[c]	2.49 ± 0.04 [a]	4.76 ± 0.19 [c]	10.21 ± 0.30[d]	21.78 ± 0.55[d]	32.57 ± 0.69[d]
CS-CRE5	0.09 ± 0.001[d]	2.27 ± 0.06 [a]	4.23 ± 0.18 [c]	8.43 ± 0.26[e]	16.51 ± 0.48[e]	28.19 ± 0.57[e]

bacteria cell membranes [57]. There are certain compounds present in the CRE like phenolic acids, sulfur-containing compounds (diallyl sulfides), flavonoids and allicin, which are responsible for the antimicrobial activity [58]. Antimicrobial potential of phenolic compounds is the result of physiological changes occurring in the cell membrane of bacterium, which ultimately led to cell death [59]. Furthermore, allicin present in CRE is responsible for reactions between thiol groups and thiosulfinates and resulted in inactivation of thiolic enzymes present in bacteria and production of allyl-disulfides, which further modified the L-cysteine leading to bacterial death [19]. Similar antimicrobial behavior of CS films incorporated with turmeric extract has been reported earlier [60].

3.5.3. Biodegradation evaluation

The results of biodegradation of CS and CS-CRE films are presented in Fig. 4C. An increase ($p < 0.05$) was observed in a weight loss of CS control film and CS-CRE films. The weight loss was gradually increased for all the tested film as the time of soil dumping was increased to three weeks. The CS-CRE5 film exhibited the highest weight loss of 47.36% after 3 weeks, whereas for CS control film, it was 26.98%. A similar trend of biodegradation was reported when rosemary extract [61] and yerba extract [62] were added to the cassava-starch film. The prominent outcome of the biodegradation evaluation in this study is that the addition of the CRE into CS films improved biodegradability due to the formation of new polymeric materials and putting lesser burden on the environment by quick degradation.

3.6. Potential application on soybean oil packaging

3.6.1. Oil resistance ability of films

The oil resistance ability of CS-based CRE films as a potential application for food packaging was evaluated by the OAR. The results showed that CS-CRE5 film exhibited lower OAR compared to the CS control film (Table 5). There was a significant decrease in OAR that was observed in CS-CRE1, CS-CRE3 and CSMC-CRE5 films. The possible reason behind this decrease is the presence of hydrophilic hydroxyl groups in the structure of CS and the addition of CRE lead to the increased thickness of the films, which made it difficult for oil molecules to pass through the films. Thus, the low values of OAR showed a higher oil resistance ability, which is a desirable trait for the packaging material for oil products.

3.6.2. Peroxide value (POV)

POV is a convenient and most widely used method to determine the oxidation and rancidity of the oil caused by the saturation of unsaturated fatty oxides [63]. The results of the POV of soybean oil stored for 28 days are presented in Table 5. The CS-based CRE films showed a significant reduction in the oxidation of the oil. All treatments resulted in an increased POV regardless of the time, but this increase of POV was slower with CS-CRE films as compared to open control and CS film. On the 28th day of storage, open control has the highest value of POV 69.23 ± 1.38 (mEq/kg) while for CS-CRE5 it was 31.16 ± 1.43 (mEq/kg). The compact structure of the bio-composite film played a vital role in the reduction of oxidation by making oxygen difficult to pass through [64]. Furthermore, the antioxidant capacity of the film was increased by the presence of phenolic compounds in the film, which also contributed to slow the oxidation of the oil. Hence, it can be inferred that CS-based CRE films could be used as a packaging material for foods that are highly susceptible to oxidation.

4. Conclusion

Chinese chives root extract, which is regarded as food waste, is a good source of bioactive compounds. In this study, the effect of CRE as an active agent was explored after incorporation into the CS-based food packaging film. Physical properties of the CS film were improved in terms of moisture content, water-solubility, swelling degree and thickness by the addition of CRE. Water vapor permeability was decreased, which shows the good barrier property of CS-based CRE film. Furthermore, overall color attributes were enhanced from transparent to opaque. Additionally, CS-CRE films exhibited good antioxidant activity and possessed a higher inhibitory effect against four kinds of bacteria tested in this study. It may be inferred that CS-based CRE films have good potential to be used as an environmentally friendly food packaging film for the food industry.

CRediT authorship contribution statement

Asad Riaz: Conceptualization, Methodology, Software, Writing - original draft.**Camel Lagnika:**Conceptualization, Methodology, Data curation.**Hao Luo:**Formal analysis, Visualization, Investigation.**Zhuqing Dai:**Software, Validation.**Meimei Nie:**Methodology, Software.**Malik Muhammad Hashim:**Writing - review & editing.**Chunquan Liu:** Funding acquisition.**Jiangfeng Song:**Project administration.**Dajing Li:** Supervision, Resources.

Acknowledgment

This work was supported by the Key Research and Development Program of Jiangsu Province (BE2018382).

References

[1] J. Liu, S. Liu, Y. Chen, L. Zhang, J. Kan, C. Jin, Physical, mechanical and antioxidant properties of chitosan films grafted with different hydroxybenzoic acids, Food Hydrocoll. 71 (2017) 176–186.
[2] C.G. Otoni, R.J. Avena-Bustillos, H.M. Azeredo, M.V. Lorevice, M.R. Moura, L.H. Mattoso, Recent advances on edible films based on fruits and vegetables—a review, Compr. Rev. Food Sci. Food Saf. 16 (2017) 1151–1169.
[3] K.D. Cox, G.A. Covernton, H.L. Davies, J.F. Dower, F. Juanes, S.E. Dudas, Human consumption of microplastics, Environ. Sci. Technol. 53 (2019) 7068–7074.
[4] B. Hassan, S.A.S. Chatha, A.I. Hussain, K.M. Zia, N. Akhtar, Recent advances on polysaccharides, lipids and protein based edible films and coatings: a review, Int. J. Biol. Macromol. 109 (2018) 1095–1107.
[5] P. Cazon, G. Velazquez, J.A. Ramírez, M. Vázquez, Polysaccharide-based films and coatings for food packaging: a review, Food Hydrocoll. 68 (2017) 136–148.
[6] A. Nor Adilah, B. Jamilah, M.A. Noranizan, Z.A. Nur Hanani, Utilization of mango peel extracts on the biodegradable films for active packaging, Food Packag. Shelf Life 16 (2018) 1–7.
[7] E.M. Ciannamea, P.M. Stefani, R.A. Ruseckaite, Properties and antioxidant activity of soy protein concentrate films incorporated with red grape extract processed by casting and compression molding, LWT Food Sci. Technol. 74 (2016) 353–362.
[8] Z.A. Maryam Adilah, B. Jamilah, Z.A. Nur Hanani, Functional and antioxidant properties of protein-based films incorporated with mango kernel extract for active packaging, Food Hydrocoll. 74 (2018) 207–218.
[9] C. Medina-Jaramillo, O. Ochoa-Yepesa, C. Bernalb, L. Famá, Active and smart biodegradable packaging based on starch and natural extracts, Carbohydr. Polym. 176 (2017) 187–194.
[10] H.M. Yong, X.C. Wang, R.Y. Bai, Z.Q. Miao, X. Zhang, J. Liu, Development of antioxidant and intelligent pH-sensing packaging films by incorporating purple-fleshed sweet potato extract into chitosan matrix, Food Hydrocoll. 90 (2019) 216–224.
[11] J. Gómez-Estaca, C. López-de-Dicastillo, P. Hernández-Munoz, R. Catalá, R. Gavara, Advances in antioxidant active food packaging, Trends Food Sci. Technol. 35 (2014) 42–51.
[12] M. Dash, F. Chiellini, R.M. Ottenbrite, E. Chiellini, Chitosan-a versatile semi-synthetic polymer in biomedical applications, Prog. Polym. Sci. 36 (2011) 981–1014.
[13] H. Yong, F.C. Wang, X. Zhang, Y.P. Liu, Y. Qin, J. Liu, Effects of anthocyanin-rich purple and black eggplant extracts on the physical, antioxidant and pH-sensitive properties of chitosan film, Food Hydrocoll. 94 (2019) 93–104.
[14] X. Wang, H. Yong, L. Gao, L. Li, M. Jin, J. Liu, Preparation and characterization of antioxidant and pH-sensitive films based on chitosan and black soybean seed coat extract, Food Hydrocoll. 89 (2019) 56–66.
[15] J.F. Rubilar, M.S.C. Rui, H.D. Silva, A.A. Vicente, I. Khmelinskii, M.C. Vieira, Physico-mechanical properties of chitosan films with carvacrol and grape seed extract, J. Food Eng. 115 (2013) 466–474.
[16] T.M. Crizel, O.R. Alessandro, D.A. Vítor, B. Narcisa, M.M. Margarida, H.F. Simone, Active food packaging prepared with chitosan and olive pomace, Food Hydrocoll. 74 (2018) 139–150.
[17] A. Riaz, S. Lei, H.M.S. Akhtar, P. Wan, D. Chen, S. Jabbar, M. Abid, M.M. Hashim, X.X. Zeng, Preparation and characterization of chitosan-based antimicrobial active food packaging film incorporated with apple peel polyphenols, Int. J. Biol. Macromol. 114 (2018) 547–555.

[18] W.N. Zhang, H.L. Zhang, C.Q. Lu, J.P. Luo, X.Q. Zha, A new kinetic model of ultrasound-assisted extraction of polysaccharides from Chinese chive, Food Chem. 212 (2016) 274–281.
[19] P. Putnik, D. Gabrić, S. Roohinejad, F.J. Barba, D. Granato, K. Mallikarjunan, J.M. Lorenzo, D.B. Kovačević, An overview of organosulfur compounds from *Allium spp.*: from processing and preservation to evaluation of their bioavailability, antimicrobial, and anti-inflammatory properties, Food Chem. 276 (2019) 680–691.
[20] L.Q. Zhang, Y. Li, Y. Liang, K.H. Liang, F. Zhang, T. Xu, M.M. Wang, H.X. Song, X.J. Liu, B.Y. Lu, Determination of phenolic acid profiles by HPLC-MS in vegetables commonly consumed in China, Food Chem. 276 (2019) 538–546.
[21] Y. Zeng, Y. Li, J. Yang, X. Pu, J. Du, X. Yang, S. Yang, Therapeutic role of functional components in *Alliums* for preventive chronic disease in human being, Evid. Based Complement. Alternat. Med. 2017 (2017) 1–13.
[22] Y.C. Ma, J. Yu, J.P. Wang, L. Cai, Z.T. Ding, Chemical constituents of the roots of *Allium tuberosum*, Ch. Pharm. J. 51 (2016) 972–975.
[23] J.L. Mau, C.P. Chen, P.C. Hsieh, Antimicrobial effect of extracts from chinese chive, cinnamon, and corni fructus, J. Agric. Food Chem. 49 (2001) 183–188.
[24] M. Saeeduddin, M. Abid, S. Jabbar, T. Wu, Q.X. Yuan, A. Riaz, B. Hu, L. Zhou, X.X. Zeng, Nutritional, microbial and physicochemical changes in pear juice under ultrasound and commercial pasteurization during storage, J. Food Process. Preserv. 41 (2017), e13237.
[25] M. Hassannia-Kolaee, F. Khodaiyan, I. Shahabi-Ghahfarrokhi, Modification of functional properties of pullulan-whey protein bionanocomposite films with nanoclay, J. Food Sci. Technol. 53 (2016) 1294–1302.
[26] A. Riaz, C. Lagnika, M. Abdin, M.M. Hashim, W. Ahmed, Preparation and characterization of chitosan/gelatin based active food packaging films containing apple peel nanoparticles, J. Polym. Environ. 28 (2020) 411–420.
[27] A. Ferreira, C. Nunes, A. Castro, P. Ferreira, M.A. Coimbra, Influence of grape pomace extract incorporation on chitosan films properties, Carbohydr. Polym. 113 (2014) 490–499.
[28] J. Liu, C.G. Meng, S. Liu, J. Kan, C.H. Jin, Preparation and characterization of protocatechuic acid grafted chitosan films with antioxidant activity, Food Hydrocoll. 63 (2017) 457–466.
[29] S. Khalid, L. Yu, M.Y. Feng, L.H. Meng, Y.T. Bai, A. Ali, H.S. Liua, L. Chen, Development and characterization of biodegradable antimicrobial packaging films based on polycaprolactone, starch and pomegranate rind hybrids, Food Packag. Shelf Life 18 (2018) 71–79.
[30] D. Firestone, Association of Coaching Supervisors. Official and Recommended Practices of the American Oil Chemists' Society, Official Methods and Recommended Practices, 5th ed. AOAC Press, Champaign, IL, USA, 1998.
[31] G.F. Deng, X. Lin, X.R. Xu, L.L. Gao, J.F. Xie, H.B. Li, Antioxidant capacities and total phenolic contents of 56 vegetables, J. Funct. Foods 5 (2013) 260–266.
[32] S.F. Hosseini, M. Rezaei, M. Zandi, F. Farahmandghavi, Development of bioactive fish gelatin/chitosan nanoparticles composite films with antimicrobial properties, Food Chem. 194 (2016) 1266–1274.
[33] L. Sun, J. Sun, L. Chen, P. Niu, X. Yang, Y. Guo, Preparation and characterization of chitosan film incorporated with thinned young apple polyphenols as an active packaging material, Carbohydr. Polym. 163 (2017) 81–91.
[34] R. Akhter, F.A. Masoodi, T.A. Wani, S.A. Rather, Functional characterization of biopolymer based composite film: incorporation of natural essential oils and antimicrobial agents, Int. J. Biol. Macromol. 137 (2019) 1245–1255.
[35] C. Qiao, X. Ma, J. Zhang, J. Yao, Molecular interactions in gelatin/chitosan composite films, Food Chem. 235 (2017) 45–50.
[36] F. Bi, X. Zhang, R. Bai, Y.P. Liu, J. Liu, J. Liu, Preparation and characterization of antioxidant and antimicrobial packaging films based on chitosan and proanthocyanidins, Int. J. Biol. Macromol. 134 (2019) 11–19.
[37] L.Y. Wang, H.Y. Guo, J. Wang, G.C. Jiang, F.H. Du, X.J. Liu, Effects of *Herba Lophatheri* extract on the physicochemical properties and biological activities of the chitosan film, Int. J. Biol. Macromol. 133 (2019) 51–57.
[38] A. Ali, L. Yu, H.S. Liu, S. Khalid, L.H. Meng, L. Chen, Preparation and characterization of starch-based composite films reinforced by corn and wheat hulls, J. Appl. Polym. Sci. 134 (2017), 45159.
[39] A. Ali, F.W. Xie, L. Yu, H.S. Liu, L.H. Meng, S. Khalid, L. Chen, Preparation and characterization of starch-based composite films reinfoced by polysaccharide-based crystals, Compo. Part B: Eng. 133 (2018) 122–128.
[40] Y.Y. Zhang, Y. Yang, K. Tang, X. Hu, G.L. Zou, Physicochemical characterization and antioxidant activity of quercetin-loaded chitosan nanoparticles, J. Appl. Polym. Sci. 107 (2008) 891–897.
[41] K. Halasz, L. Csóka, Black chokeberry (*Aronia melanocarpa*) pomace extract immobilized in chitosan for colorimetric pH indicator film application, Food Packag. Shelf Life 16 (2018) 185–193.
[42] J. Hafsa, M. Smach, M.R. ali, Ben Khedher, B. Charfeddine, K. Limem, H. Majdoub, S. Rouatbi, Physical, antioxidant and antimicrobial properties of chitosan films containing *Eucalyptus globulus* essential oil, LWT Food Sci. Technol. 68 (2016) 356–364.
[43] J. Uranga, A.I. Puertas, A. Etxabide, M.T. Dueñas, P. Guerrero, K. de la Caba, Citric acid incorporated fish gelatin/chitosan composite films, Food Hydrocoll. 86 (2019) 95–103.
[44] L. Rui, X. Minhao, H. Bing, Z. Li, Y. Danyang, Z. Xiaoxiong, A comparative study on chitosan/gelatin composite films with conjugated or incorporated gallic acid, Carbohydr. Polym. 173 (2017) 473–481.
[45] U. Siripatrawan, B.R. Harte, Physical properties and antioxidant activity of an active film from chitosan incorporated with green tea extract, Food Hydrocoll. 24 (2010) 770–775.
[46] M. Kurek, I.E. Garofulić, M.T. Bakić, M. Ščetar, V.D. Uzelac, K. Galić, Development and evaluation of a novel antioxidant and pH indicator film based on chitosan and food waste sources of antioxidants, Food Hydrocoll. 84 (2018) 238–246.
[47] Y.A. Arfat, J. Ahmed, N. Hiremath, R. Auras, A. Joseph, Thermo-mechanical, rheological, structural and antimicrobial properties of bionanocomposite films based on fish skin gelatin and silver copper nanoparticles, Food Hydrocoll. 62 (2017) 191–202.
[48] L. Wang, Y. Dong, H. Men, J. Tong, J. Zhou, Preparation and characterization of active films based on chitosan incorporated tea polyphenols, Food Hydrocoll. 32 (2013) 35–41.
[49] S. Khoshgozaran-Abras, M.H. Azizi, Z. Hamidy, N. Bagheripoor-Fallah, Mechanical, physicochemical and color properties of chitosan based-films as a function of *Aloe vera* gel incorporation, Carbohydr. Polym. 87 (2012) 2058–2062.
[50] C. Pastor, L. Sánchez-González, A. Chiralt, M. Cháfer, C. González-Martínez, Physical and antioxidant properties of chitosan and methylcellulose based films containing resveratrol, Food Hydrocoll. 30 (2013) 272–280.
[51] R. Priyadarshi, B. Kumar, F. Deeba, A. Kulshreshtha, Y.S. Negi, Chitosan films incorporated with apricot (*Prunus armeniaca*) kernel essential oil as active food packaging material, Food Hydrocoll. 85 (2018) 158–166.
[52] L. Wang, Q. Wang, J. Tong, J. Zhou, Physicochemical properties of chitosan films incorporated with honeysuckle flower extract for active food packaging, J. Food Process Eng. 40 (2017) https://doi.org/10.1111/jfpe.12305(n/a-n/a).
[53] K. Rambabu, G. Bharath, F. Banat, P.L. Show, H.H. Cocoletzi, Mango leaf extract incorporated chitosan antioxidant film for active food packaging, Int. J. Biol. Macromol. 126 (2019) 1234–1243.
[54] T.B. Dey, S. Chakraborty, K.K. Jain, A. Sharma, R.C. Kuhad, Antioxidant phenolics and their microbial production by submerged and solid state fermentation process: a review, Trends Food Sci. Technol. 53 (2016) 60–74.
[55] N. Hari, S. Francis, A.G.R. Nair, A.J. Nair, Synthesis, characterization and biological evaluation of chitosan film incorporated with β-carotene loaded starch nanocrystals, Food Packag. Shelf Life 16 (2018) 69–76.
[56] Y.H. Wu, X.G. Luo, W. Li, R. Song, J. Li, Y. Li, B. Li, S. Liu, Green and biodegradable composite films with novel antimicrobial performance based on cellulose, Food Chem. 197 (2016) 250–256.
[57] X. Zhang, Y. Liu, H. Yong, Y. Qin, J. Liu, J. Liu, Development of multifunctional food packaging films based on chitosan, TiO2 nanoparticles and anthocyanin-rich black plum peel extract, Food Hydrocoll. 94 (2019) 80–92.
[58] M. Snoussi, N. Trabelsi, A. Dehmeni, R. Benzekri, L. Bouslama, B. Hajlaoui, A. Papetti, Phytochemical analysis, antimicrobial and antioxidant activities of *Allium roseum* var. *odoratissimum* (*Desf.*) Coss extracts, Ind. Crop. Prod. 89 (2016) 533–542.
[59] A. Ali, Y. Chen, H.S. Liu, L. Yu, Z. Baloch, S. Khalid, J. Zhu, L. Chen, Starch-based antimicrobial films functionalized by pomegranate peel, Int. J. Biol. Macromol. 129 (2019) 1120–1126.
[60] Z. Kalaycıoğlu, E. Torlak, G. Akın-Evingür, İ. Özen, F.B. Erim, Antimicrobial and physical properties of chitosan films incorporated with turmeric extract, Int. J. Biol. Macromol. 101 (2017) 882–888.
[61] D. Piñeros-Hernandez, C. Medina-Jaramillo, A. López-Córdoba, S. Goyanes, Edible cassava starch films carrying rosemary antioxidant extracts for potential use as active food packaging, Food Hydrocoll. 63 (2017) 488–495.
[62] C. Medina Jaramillo, P.G. Seligra, S. Goyanes, C. Bernal, L. Famá, Biofilms based on cassava starch containing extract of yerba mate as antioxidant and plasticizer, Starke 67 (2015) 780–789.
[63] R. Farhoosh, S. Einafshar, P. Sharayei, The effect of commercial refining steps on the rancidity measures of soybean and canola oils, Food Chem. 115 (2009) 933–938.
[64] L. Mariniello, C.V. Giosafatto, P.P. Di, A. Sorrentino, R.J. Porta, Swelling, mechanical, and barrier properties of albedo-based films prepared in the presence of phaseolin cross-linked or not by transglutaminase, Biomacromol 11 (2010) 2394–2398.